DEVELOPMENT OF OPTIMIZED, GRADED-PERMEABILITY AXIAL GROOVE HEAT PIPES

Michael R. Kapolnek and H. Rolland Holmes
Lockheed Missiles and Space Company, Inc.

ABSTRACT

Heat pipe performance can usually be improved by uniformly varying or "grading" wick permeability from end to end. This paper describes a unique and cost-effective method for grading the permeability of an axial groove heat pipe: selective chemical etching of the pipe casing. This method was developed and demonstrated on a proof-of-concept test article. The process improved the test article's performance by 50 percent. Further improvement is possible through the use of optimally etched grooves.

INTRODUCTION

Grading the permeability of simple, nonarterial wicks has previously been shown to improve heat pipe performance. An axial groove heat pipe consisting of pipe segments with different groove geometries is one way in which this has been done (ref. 1). Graded porosity slab wicks (ref. 2) use the same principle but are more difficult and costly to fabricate than axial groove designs. This paper describes a new method for grading the permeability of an axial groove heat pipe.

The new method is based on variable chemical etching of the grooves so that the amount of material removed varies along the length of the pipe. Such a method is cost-effective and can substantially increase the heat pipe performance while slightly decreasing the weight. This improvement extends the weight-effective range of axial groove heat pipes to higher power applications, providing even more extensive usage of this flight-proven design.

SYMBOLS

Values are given in both SI and U.S. Customary Units. The measurements and calculations were made in U.S. Customary Units.

A	Area
d_L	Liquid diameter
K	Permeability
L_p	Length of the heat pipe
$\dot{m}$	Mass flow rate
N	Number of calculation subintervals
Δp_L	Liquid pressure loss
Δp_V	Vapor pressure loss

r	Effective capillary radius
r_c	Effective capillary radius at the heat pipe condenser end
r_{min}	Minimum effective capillary radius
R_t	Fin tip radius
t_{etch}	Thickness reduction due to chemical etching
x	Distance along heat pipe measured from condenser end
μ	Liquid viscosity
ρ	Liquid density
σ	Surface tension
θ	Groove angle

CONCEPT

The thermal transport of axial groove heat pipes is generally limited by capillary pumping. The capillary transport limit is reached when the total of the liquid and vapor pressure losses at any location along the heat pipe length is equal to the local maximum available capillary pumping head (Figure 1). The capillary pressure head is created by the liquid/vapor meniscus at the groove slot and is inversely proportional to the radius of curvature of this meniscus. Figure 2 shows a cross-section of a typical groove, where this radius is specified as r_{min}. The maximum capillary head is, therefore, limited by the smallest capillary radius that can form in the given groove geometry. The performance of the pipe can be maximized by creating a small groove width at the liquid-vapor interface (which allows the formation of a meniscus with a small radius of curvature) and a large flow area in the groove.

This small groove width is not required over the entire pipe length to optimize performance. A small meniscus radius will only occur where large liquid/vapor pressure differences exist; small groove widths are only beneficial at these locations. A small meniscus radius generally occurs near the evaporator end of the pipe. Large liquid areas are desirable at all locations in order to minimize frictional flow losses. Since the groove area is directly related to the groove width, the performance of the pipe can be optimized by varying the groove size so that it is just small enough to support the meniscus that will form at any given point. In general, this will result in large open grooves in the condenser portion of the pipe and smaller grooves in the evaporator.

This new concept uses chemical etching to tailor the geometry of axial grooves along the heat pipe length. Chemical etching is a commonly used machining process. The amount of material etched is directly proportional to the time in the etchant as well as the concentration of etchant and its temperature. Of these three independent variables, exposure time is the easiest to control. The axial groove wick can be graded by controlling the exposure time of each axial location along the heat pipe.

This concept was developed as an alternative to the use of multiple cross sections for varying the groove geometry of axial groove heat pipes. The new process has two main advantages. With a well-controlled grading process, the groove profile can be optimized for any given application. Also, a single heat pipe casing is used, greatly simplifying the fabrication process.

DESIGN ANALYSIS

A computer code (GGROOVE), capable of calculating the capillary transport limit of axial groove heat pipes with lengthwise-varying cross sections, was developed to analyze alternate grading profiles. The number and shape of the unetched axial grooves are input to the code, along with the equation that defines the etching profile. Input to GGROOVE also includes the vapor section shape, working fluid, operating temperature, and gravity constant. The code then iterates on the heat transport of the pipe until the total pressure drop (liquid and vapor) at any point in the pipe equals the available capillary head at that point. The working fluid charge quantity is also calculated by the code.

The code uses a bisection technique to iterate on heat transport until a local meniscus radius of curvature has been minimized at a point x within the heat pipe. By balancing local capillary pressure head with flow losses, an expression for the local meniscus radius of curvature, r(x), results:

$$\Delta p_L(x) + \Delta p_V(x) + 2\sigma \left(\frac{1}{r(x)} - \frac{1}{r_c} \right) = 0 \tag{1}$$

$$r(x) = 1 \Big/ \left(\frac{1}{r_c} - \frac{\Delta p_L(x) + \Delta p_V(x)}{2\sigma} \right) \tag{2}$$

where r_c is the effective capillary radius at the condenser end of the pipe. Gravity-induced flow losses have been neglected to simplify the discussion.

Viscous flow losses in the axial grooves are evaluated using Darcy's Law (ref. 3):

$$\frac{dp_L}{dx} = -\frac{\mu \dot{m}}{\rho K A} \tag{3}$$

The groove permeability, K, and total wick flow area, A, are dependent on the shape of the grooves. Since the groove shape varies with location, the permeability and flow area also depend on location. Because evaporation and condensation occur, the total mass flow through the grooves, $\dot{m}$, is location dependent. The mass flow rate is calculated using the heat transport and the latent heat of the working fluid.

Integrating both sides of Equation 3:

$$\Delta p_L = \int_0^L -\frac{\mu}{\rho} \frac{\dot{m}(x)}{K(x) A(x)} dx \tag{4}$$

the integral can be approximated by

$$\Delta p_L \approx -\frac{\mu}{\rho} \sum_{i=1}^N \frac{\dot{m}(w_i)}{K(w_i) A(w_i)} \Delta x \tag{5}$$

where w_i is a number within the subinterval [x_{i-1}, x_i]. A(x), K(x) and $\dot{m}(x)$ are assumed to be constant within the subinterval, an assumption that improves as the subinterval size decreases. The GGROOVE

399

code evaluates $\dot{m}$, A, and K at the x_j end of each subinterval. The number of subintervals, N, is input by the user and is typically about 1000. The viscous flow loss in the liquid wick from the condenser end of the pipe through subinterval j is then

$$\Delta p_L\left(x_j\right) = -\frac{\mu}{\rho} \sum_{i=1}^{j} \frac{\dot{m}\left(x_i\right)}{K\left(x_i\right) A\left(x_i\right)} \frac{L_P}{N}$$

(6)

Because the vapor pressure loss, $\Delta p_v(x_j)$, is typically 10 percent or less of the total pressure loss for an axial groove heat pipe, the effect of varying geometry on it is negligible. This allows the use of closed-form expressions for its calculation. These expressions are available in other sources (ref. 3) and are not discussed here.

The local meniscus radius, $r(x_j)$, is minimized when the geometry of the heat pipe can support no smaller value. For the axial groove geometry shown in Figure 2, the minimum effective capillary radius r_{min} is:

$$r_{min} = d_L \sin\theta - 2R_t$$

(7)

The fin tip radius, R_t, will vary with the amount of material etched, so the expression for the local minimum capillary radius is:

$$r_{min}\left(x_j\right) = d_L \sin\theta - 2R_t\left(x_j\right)$$

(8)

The capillary transport limit found by GGROOVE is the maximum heat input at which a local meniscus radius is equal to the minimum effective capillary radius. The local meniscus radius is calculated using Equation 2; the minimum effective capillary radius is calculated using Equation 8. The meniscus radii are compared at each subinterval.

The performance of a proof-of-concept test article was predicted by GGROOVE for several proposed etching profiles (Figure 3). These profiles were chosen because they could be obtained with available equipment. The etching was limited to 0.127 mm (5 mils) to ensure that no part of any groove would be completely etched away. Profile A yielded the best performance improvement (Figure 4) and was chosen as the design profile for the proof-of-concept test article. The test article was a 27-groove heat pipe, 167.6 cm (66 in.) long and approximately 1.25 cm (0.5 in.) in diameter. The article was tested prior to groove grading to obtain a performance baseline.

Subsequent to fabrication of the test article, GGROOVE was modified to permit optimization of the grading profile for a given pipe configuration. The most significant change is that the etching profile is set by an optimization routine rather than input by the user. For each subinterval j, Equation 2 is used to find the capillary radius, $r(x_j)$, required to overcome the liquid pressure losses in subintervals 1 through j-1. The maximum thickness of material that can be removed while still supporting that radius is then found using Equation 8 and the variation of $R_t(x_j)$ with etching:

$$R_t\left(x_j\right) = R_t\left(L_P\right) - t_{etch}\left(x_j\right)$$

(9)

$$r\left(x_j\right) = d_L \sin\theta - 2\left(R_t\left(L_P\right) - t_{etch}\left(x_j\right)\right)$$

(10)

$$t_{etch}\left(x_j\right) = \frac{r\left(x_j\right)}{2} + R_t\left(L_P\right) - \frac{d_L}{2}\sin\theta$$

(11)

The thickness of material etched, $t_{etch}(x_j)$, is then used to find the local groove shape as defined in Figure 2. The local permeability, $K(x_j)$, and flow area, $A(x_j)$, are calculated and used in Equation 6 to determine the liquid pressure drop $\Delta p_L(x_j)$. The capillary transport limit is found by the same method used in the original version. The code also outputs the optimum etching profile at that limit.

An optimized grading profile was found for the test article and is shown in Figure 5. It is very similar to the test article's design profile and yields a predicted performance that is the same (within the accuracy of the code).

DEVELOPMENT ARTICLE FABRICATION

The fabrication of the proof-of-concept heat pipe followed standard Lockheed heat pipe manufacturing procedures except for the addition of the etching step. A standard, on-site chemical etching facility was used. The procedure included masking of the flange, exposure to 90° C (194°F) sodium hydroxide, and several rinse steps.

A number of trial runs were conducted before attempting to etch the proof-of-concept article. Initially, several 12.5 cm (5 in.) long extrusion samples were uniformly etched for varying times in order to calibrate the solution and to assess the uniformity of the etched grooves. Examination of these samples showed the etching to occur uniformly throughout the cross section and at a rate of 0.015 mm/min (0.6 mils/min). The etched surfaces were no longer smooth but were covered with very small ripples. Because the liquid flow rate in axial groove heat pipes is highly laminar, this roughness was considered insignificant.

The next trial was on a 152 cm (60 in.) long extrusion similar to the test article. The extrusion was mounted in a basket perpendicular to the etching solution surface. The basket and pipe were lowered into the bath so that half the pipe was rapidly immersed. The rate of descent was then slowed so that the remainder of the pipe would be etched to the desired grading profile.

Two problems occurred with this trial run. First, the reaction between the aluminum and sodium hydroxide was so violent that the reaction products forced unspent etching solution through the top of the extrusion. This resulted in etching above the surface of the bath. In fact, so much etchant was expelled that the extrusion was etched nearly uniformly throughout its length.

An associated problem was that the strength of the bath was higher than in earlier calibration runs, causing too much material to be etched from the pipe. Thereafter, the strength of the etchant bath was calibrated just before each subsequent run.

The first problem was more difficult to solve. Two approaches were taken. First, the temperature of the bath was lowered to 71° C (160°F). This reduced but did not eliminate the secondary etching. The bath temperature could not be lowered further because of facility restrictions.

The second solution was to insert a 0.64-cm (0.25-in.) solid, stainless steel rod in the vapor section of the pipe before etching. Its purpose was to block etchant from rising above the surface of the bath. This further reduced etching above the bath surface but did not totally stop it. Photomicrographs of sample heat pipe sections also indicated that the circumferential etching of the grooves was not uniform.

Considering the trial runs, we decided to grade the development test article with this procedure using a larger diameter rod. The procedure in detail was :

- After cutting the end caps off the test article, an 84 cm (33 in.) long, 0.79 cm (0.3125 in.) diameter stainless steel rod was inserted into the pipe and mechanically attached at the evaporator end. The flanges of the pipe were painted with a masking compound to prevent etching.

- The pipe was mounted in a basket perpendicular to the etchant bath surface with the evaporator end facing up. The basket was then quickly lowered into the bath until 84 cm (33 in.) of the pipe were submerged.

- The descent rate of the pipe was slowed to 15.3 cm/min (6 in./min). Descent continued until 10.2 cm (4 in.) of the pipe remained outside the bath. The pipe was then rapidly removed from the bath and put through the rinsing procedure.

- The masking paint was removed from the pipe flanges; the pipe was cleaned according to standard procedures, welded closed, and charged with ammonia. The heat pipe was then ready for performance testing.

PERFORMANCE TESTING

The heat pipe evaporator and condenser configurations were the same as assumed for the design analysis. The pipe was mounted on a test stand and instrumented with 15 thermocouples. Nichrome heater tape was affixed to the pipe to heat the evaporator section. Cooling at the condenser end of the pipe was provided by 66 cm long axial groove extrusions supplied with tap water and clamped to the pipe. The test set-up is shown in Figure 6.

The heat pipe's transport limit was found with the pipe level and under four adverse tilts. The charge level was then changed and the variation of transport limit with adverse tilt redetermined. Testing was done for multiple-charge levels, because the optimum charge of the pipe could not be calculated until the exact grading profile was determined.

After testing was completed, the pipe was sectioned and photomicrographed in order to determine the actual grading profile. Sample photomicrographs are shown in Figure 7. The actual and desired profiles were then compared (Figure 8). A significant difference between them indicates that the etching procedure used did not adequately control the grading of the wick.

The actual grading profile was input to GGROOVE to determine the theoretical transport limit and optimum charge quantity. The performance of the test article at its optimum charge is compared with its theoretical performance and its performance before etching in Figure 9. Agreement between actual and theoretical performance is good. Most noteworthy, however, is the 50-percent performance improvement that resulted from the graded etching of the axial grooves.

CONCLUSIONS

The work described in this paper shows the significant benefits of this graded axial groove heat pipe concept. A significant performance improvement was demonstrated even though the etching profile achieved deviated from the design profile. By starting with an extrusion shape that has been optimized for this concept and using a better controlled etching process, much higher improvements can be achieved.

REFERENCES

1. Schlitt, K. R., "Development of an Axially Grooved Heat Pipe with Non-constant Groove Width," 3rd AIAA International Heat Pipe Conference, Paper No. 78-375, May, 1978.

2. Eninger, James, "Graded Porosity Heat Pipe Wicks," 11th AIAA Thermophysics Conference, Paper No. 76-480, July, 1976.

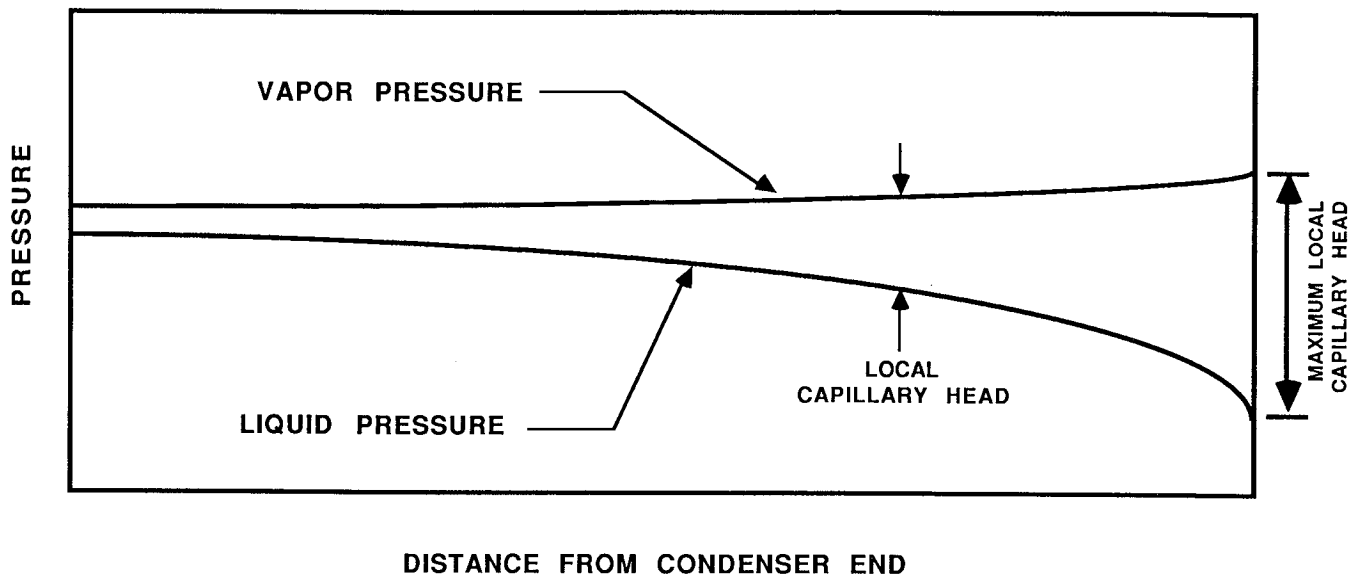3. Brennan, Patrick J. and Kroliczek, Edward J., "Heat Pipe Design Handbook," NASA Contract NAS5-23406, June, 1979.
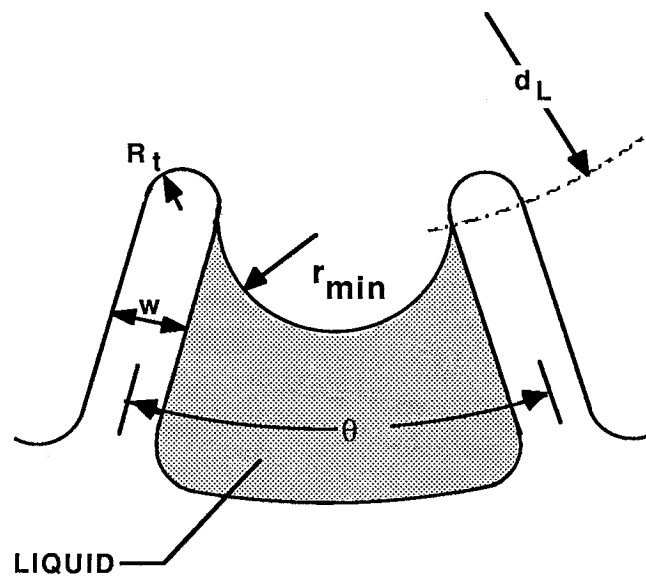
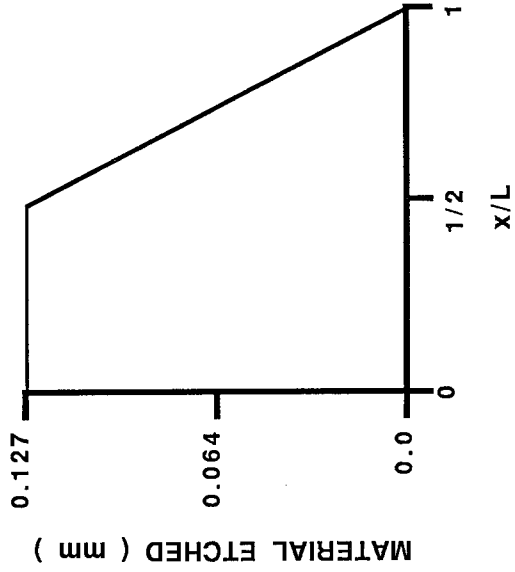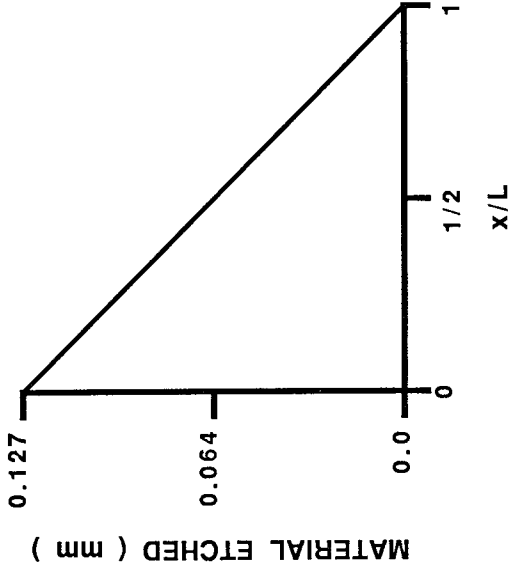**Figure 1 - Heat Pipe Pressure Distribution at Capillary Pumping Limit**

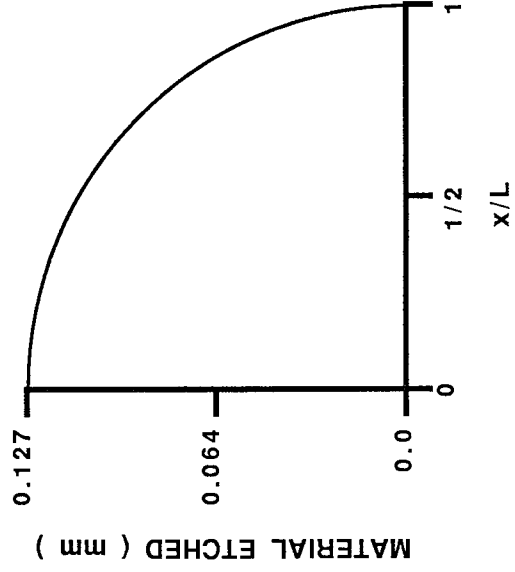**Figure 2 - Axial Groove Geometry**

Figure 3 - Candidate Etching Profiles

404

PROFILE	TRANSPORT LIMIT (W)
UNETCHED	144
A	261
B	220
C	245
D	216

ASSUMES:
0.0 cm TILT
AMMONiA WORKING FLUID
20 C OPERATING TEMPERATURE
81.3 cm EVAPORATOR
20.3 cm TRANSPORT SECTION
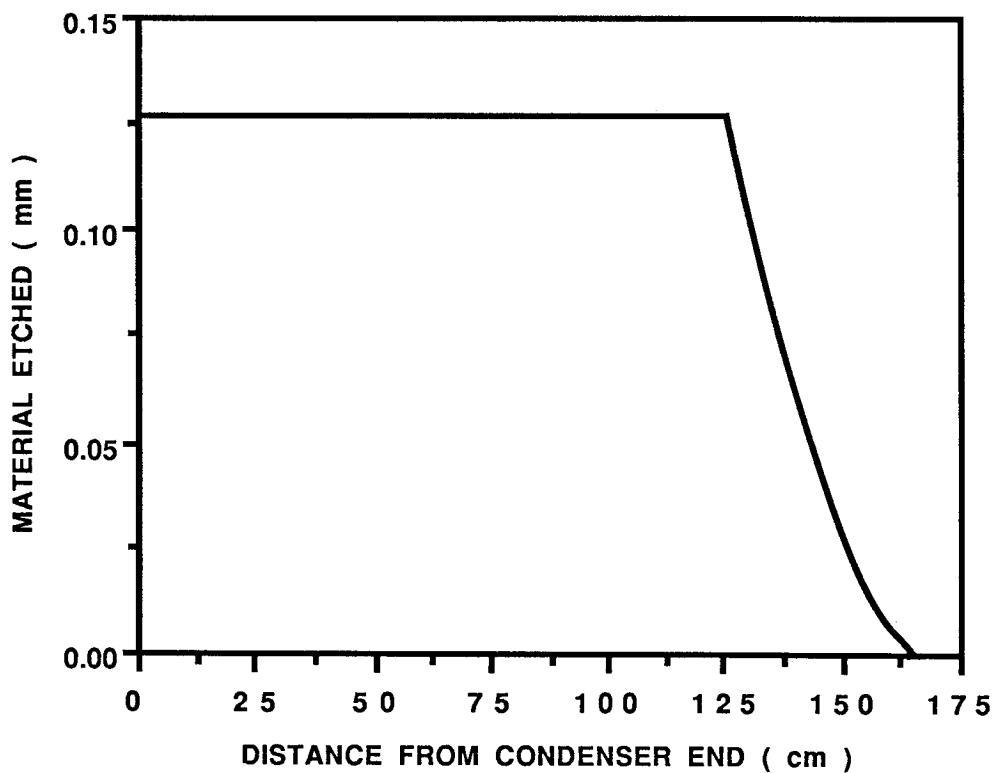66.0 cm CONDENSER

Figure 4 - Etching Profile Analysis Results
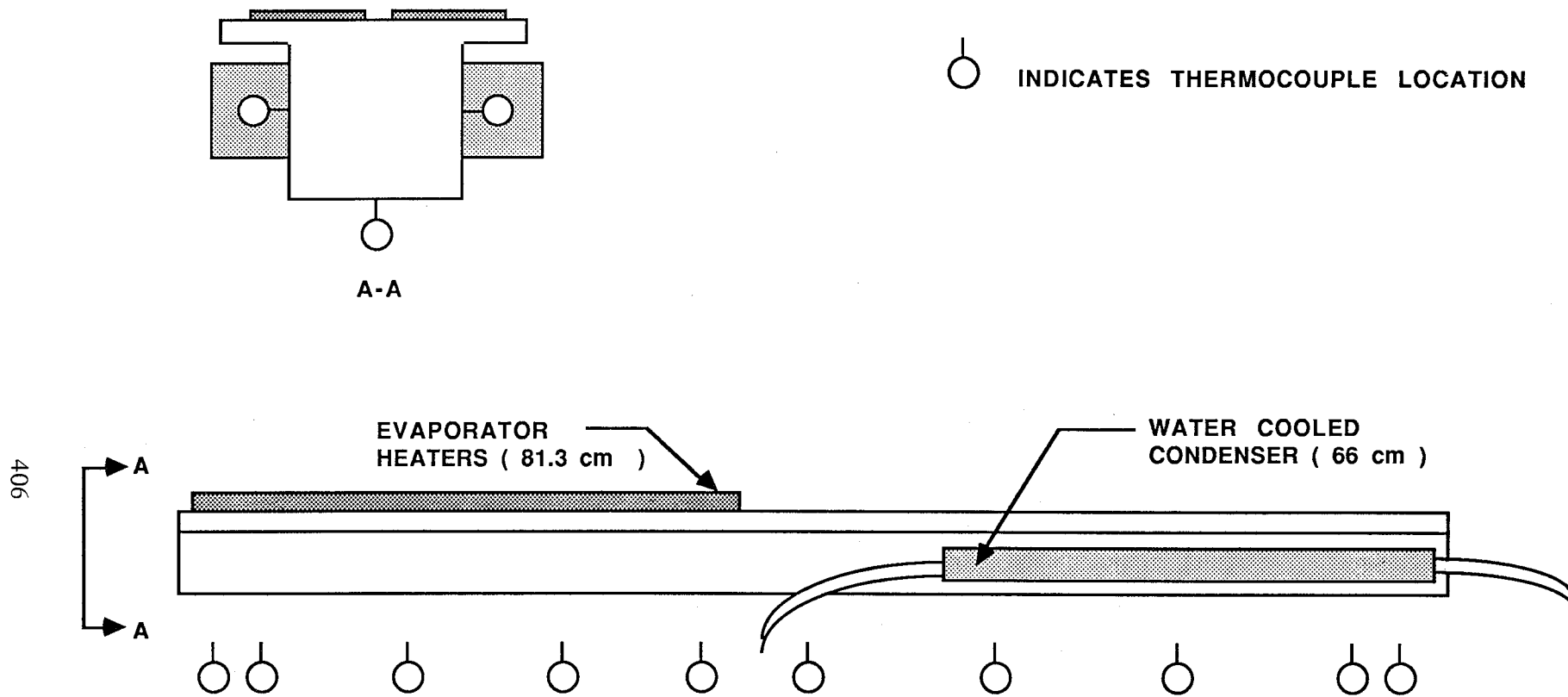

Figure 5 - Optimum Etching Profile

A-A

INDICATES THERMOCOUPLE LOCATION

EVAPORATOR HEATERS (81.3 cm)

WATER COOLED CONDENSER (66 cm)

A

A

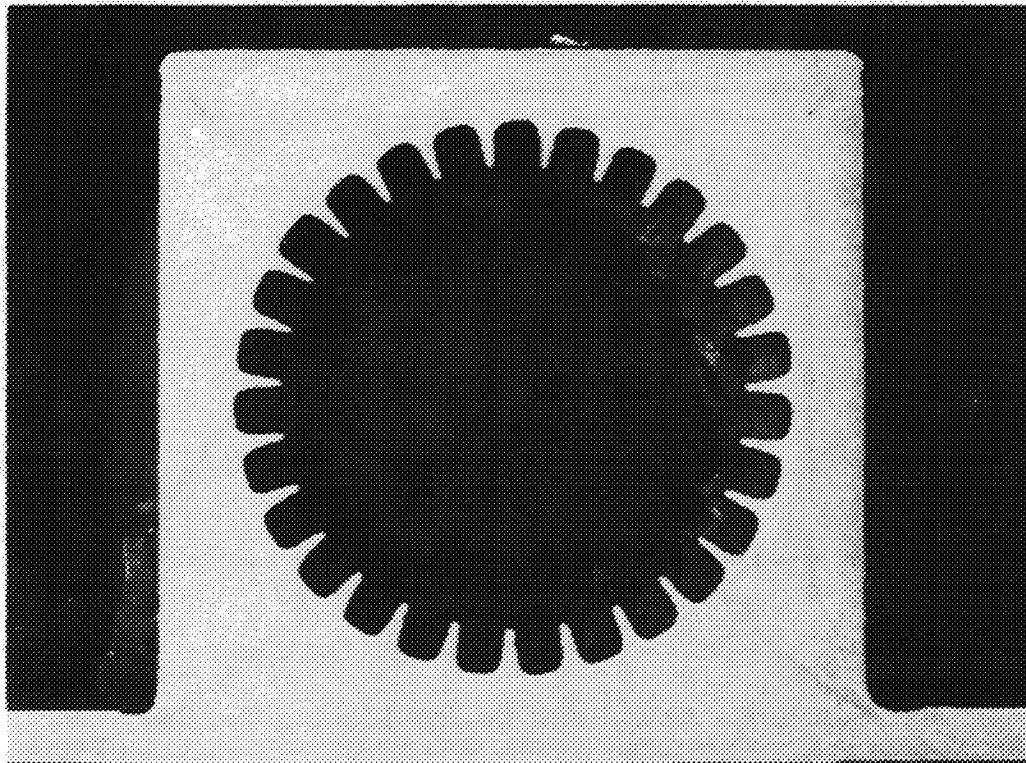Figure 6 - Bench Test Set-up

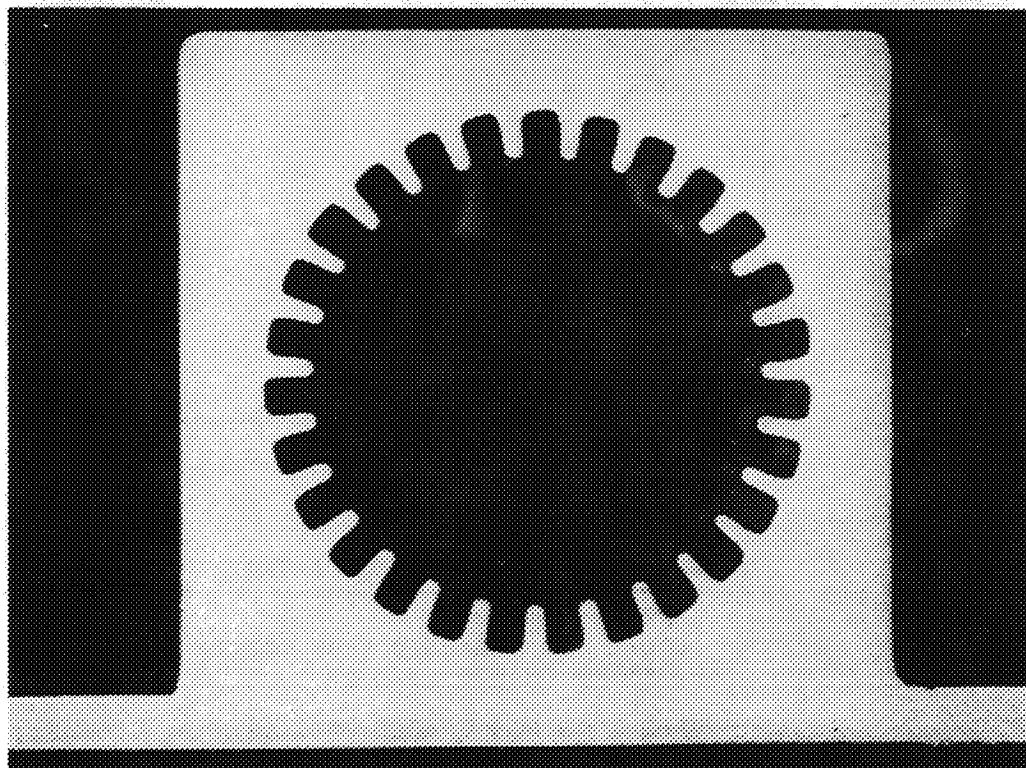**Figure 7a - Sample Photomicrograph, Condenser End**
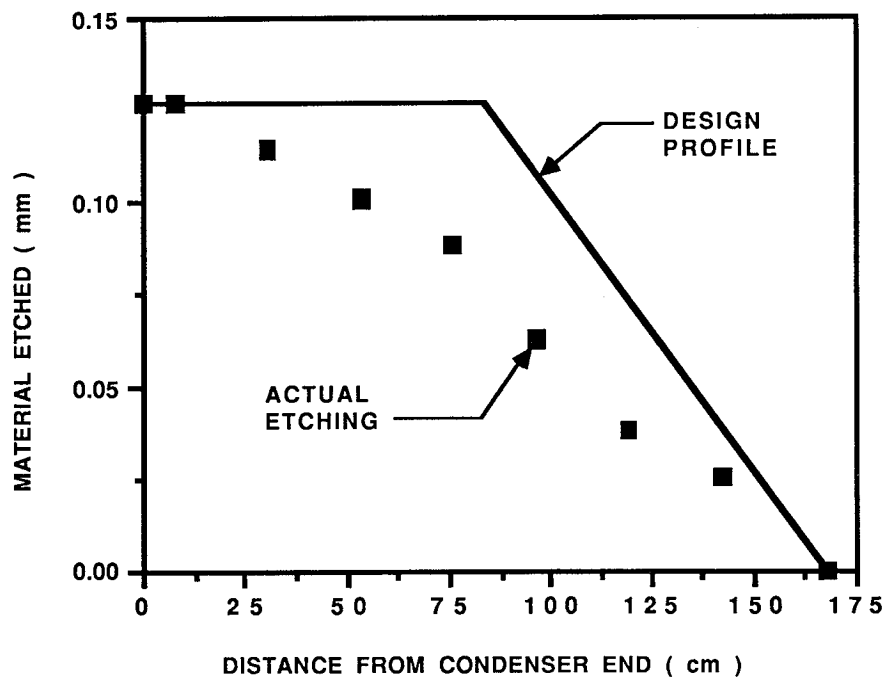

Figure 7b - Sample Photomicrograph, Evaporator End

Figure 8 - Actual and Design Etching Profiles

■ ACTUAL FOR GRADED TEST ARTICLE
(AMMONIA CHARGE = 21.9 g)

◆ ACTUAL FOR UNGRADED TEST ARTICLE
(AMMONIA CHARGE = 17.5 g)
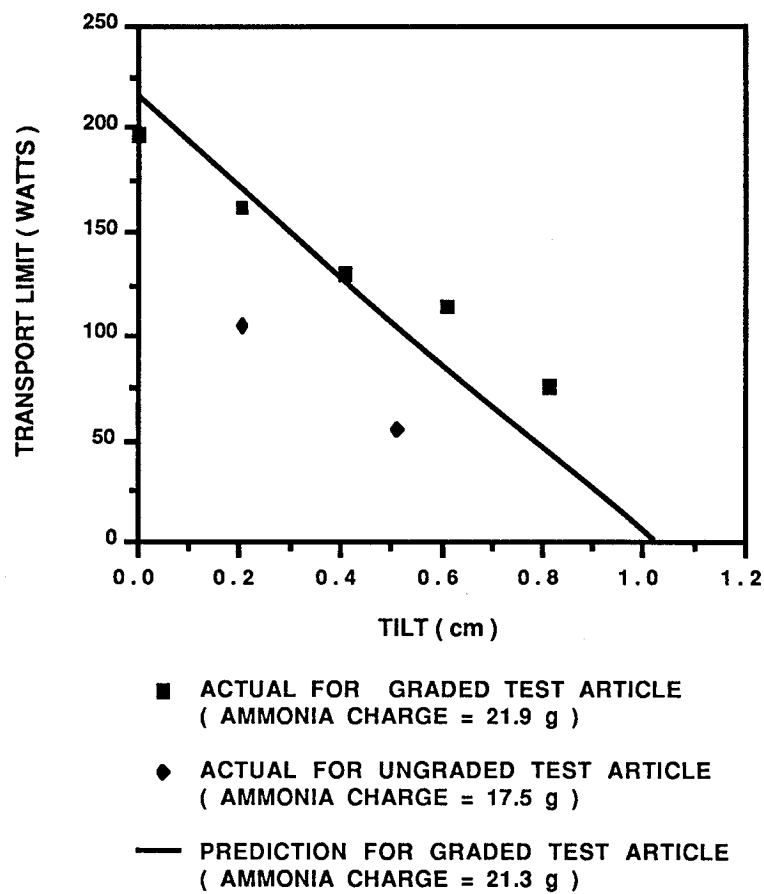
── PREDICTION FOR GRADED TEST ARTICLE
(AMMONIA CHARGE = 21.3 g)

Figure 9 - Performance of the Test Article